Supporting information

Novel metalloporphyrin covalently functionalized polyphosphazene nanotubes for boosting hydrogen evolution reaction

Xin Yang[a], Wei Zhao*[,b], Aijian Wang*[,a], Xiaoyu Zhai[a], Yuqin Dou[a], Kamal Syed[a], Weihua Zhu*[a]

[a] School of Chemistry & Chemical Engineering, Jiangsu University, Zhenjiang 212013, P.R. China

[b] School of Energy & Power Engineering, Jiangsu University, Zhenjiang 212013, P. R. China

Corresponding Author. Tel: +86-511-88791928. E-mail: wajujs@ujs.edu.cn; wzhao@ujs.edu.cn

Experimental section

Reagents and materials

All chemicals and reagents are of analytical grade and can be used without further purification. 4,4'-sulfonyldiphenol (BPS, 99.8%) and hexachlorocyclotriphosphazene (HCCP, 99%) were purchased from Adamas Reagent Co., Ltd. (Shanghai, China). Cobalt chloride ($CoCl_2$), Cesium carbonate (Cs_2CO_3), Tetrahydrofuran (THF), triethylamine (TEA) and other reagents were all bought from Sinopharm Chemical Reagent, Shanghai Co., Ltd.

Synthesis of PZSNT

Briefly (Scheme 1), HCCP (250 mg, 0.72 mmoL) and BPS (540 mg, 2.16 mmoL) were dissolved into 60 mL THF in a 250 mL three-necked flask. After ultrasonic irradiation for 30 min, TEA (435 mg, 4.32 mmol) was injected into above solution. The solution was then allowed to react for 12 h at room temperature under ultrasonic irradiation (50 W, 40 kHz). The yielded solid was filtrated and then washed three times with THF and deionized water, and then dried under vacuum for 12 h to afford the desired PZSNT. The yield was about 75%, calculated from HCCP.

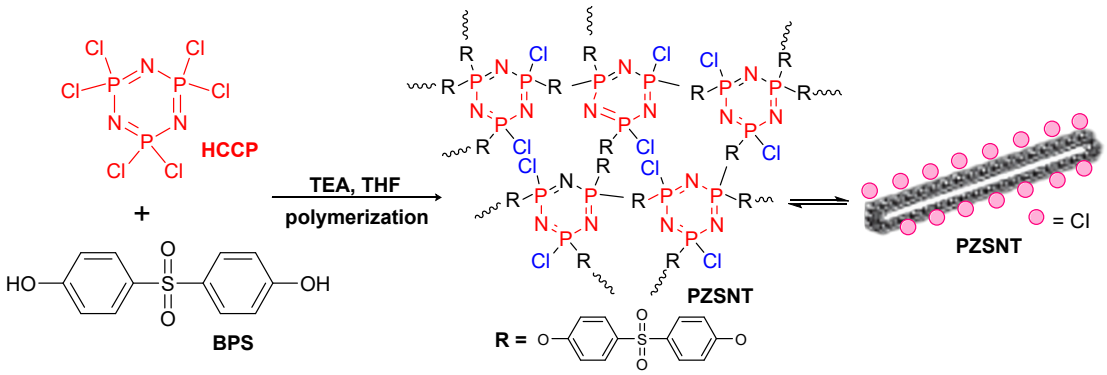

Scheme 1. Synthetic route of PZSNT.

Preparation of MTPP-PZSNT (M = Co and Ni)

To prepare MTPP-PZSNT hybrid materials, MTPP (40 mg), PZSNTs (50 mg) and Cs_2CO_3 (80 mg) were placed in a 150 mL flask. A mixed solution of THF and ethanol (50 mL) with a 1:1 volume ratio was added and the mixture was sonicated for 0.5 h to obtain a uniform suspension. The mixture was then heated to reflux and allowed to react for 48 h. Finally, the reaction mixture was cooled to room temperature, filtered under vacuum, and washed with deionized water and ethanol until the filtrate became colorless. The resultant solid was then vacuum-dried at 60 °C for 1 h to obtain the desired MTPP-PZSNT product.

Characterization

The morphology and composition analysis of the as-prepared samples were characterized by Hitachi S4800 scanning electron microscope (SEM) equipped with with the X-ray energy spectrometer (EDS) at an accelerating voltage of 120 kV. The Ultraviolet-visible (UV-vis) absorption spectra of the samples were measured with the Varian Cary 500 spectrophotometer in the range of 200-800 nm. The structure of the samples was characterized by the Fourier transform infrared (FTIR) spectrometer (Bomem, Canada) in the range of 400-4000 cm^{-1}. The surface element composition and binding energy of the prepared samples were recorded by X-Ray photoelectron spectroscopy (XPS) using a Kratos AXIS Ultra DLD-600W XPS scanning X-ray microprobe.

Electrochemical measurements

All electrochemical tests, including HER and cyclic voltammetry (CV) data,

were performed on the CHI 614E Electrochemical Workstation (Chinese CH instrument) using 1.0 M KOH and 0.5 M H_2SO_4 as the electrolytes in an H-type electrolytic cell, and the solutions were bubbled with N_2 for 0.5 h before analysis. All electrochemical measurements were recorded by using the platinum foil and catalysts covered nickel foam (NF) as the counter and working electrodes, respectively. Mercury/mercury oxide (Hg/HgO) and saturated Ag/AgCl are used as the reference electrodes in 1.0 M KOH and 0.5 M H_2SO_4 solutions, respectively. All reference electrodes were calibrated before electrochemical measurement. The final potential was converted into the reversible hydrogen electrode (RHE) by the relevant Nernst equations, i.e. $E_{RHE} = E_{Hg/HgO} + 0.0592\ pH + 0.098$ in 1.0 M KOH and $E_{RHE} = E_{Ag/AgCl} + 0.0592\ pH + 0.199$ in 0.5 M H_2SO_4. Linear sweep voltammetry (LSV) was used to determine the polarization curve of the samples and to evaluate the HER activity of the samples with a scan rate rate of 2 mV s^{-1}. The long-term durability of CoTHPP-PZSNT was evaluated in the same electrolytic cell by the chronoamperometry method at a constant potential of -0.2 V vs RHE. The yield of H_2 in a constant potential electrolysis experiments was measured using the water displacement method. Electrochemical impedance spectroscopy (EIS) measurements were performed in the frequency range of 10^5-10^{-2} Hz to evaluate the charge transfer capability of the prepared sample. At different scan rates of 20-100 mV/s, the non-Faraday double layer capacitance (C_{dl}) of the samples was collected using CV data to estimate the electrochemical surface area (ECSA).

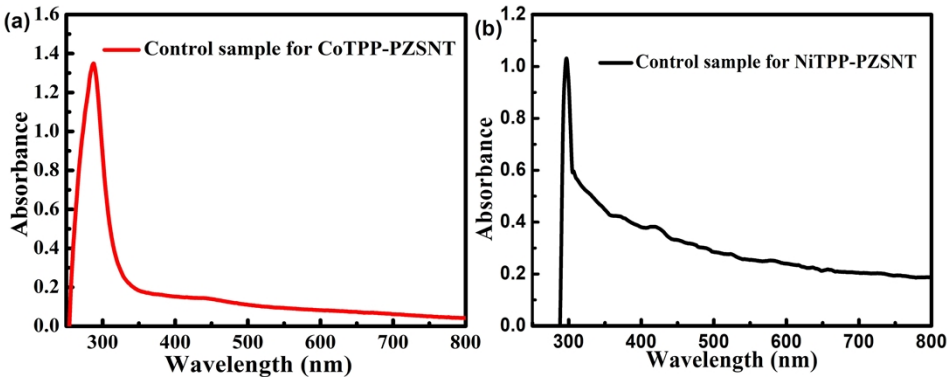

Figure S1. UV-vis absorption spectra of the control samples obtained without the acid binding agent Cs_2CO_3.

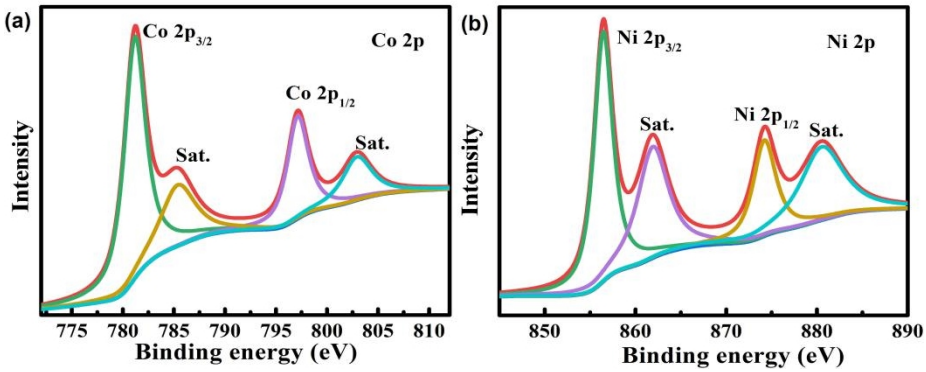

Figure S2. Sections of XPS spectra showing the (a) Co 2p of CoTPP-PZSNT, and (b) Ni 2p of NiTPP-PZSNT.

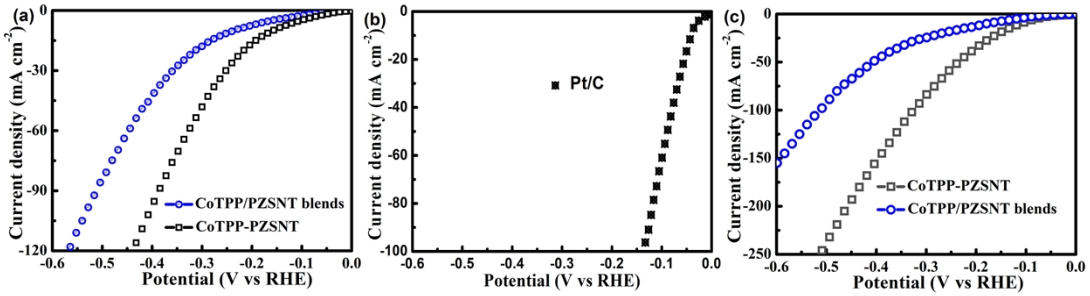

Figure S3. (a) HER LSV curves of CoTPP-PZSNT and CoTPP/PZSNT blends in 1.0 M KOH, (b) HER LSV data of commercial Pt/C, and (c) HER LSV curves of CoTPP-PZSNT and CoTPP/PZSNT blends in 0.5 M H_2SO_4.

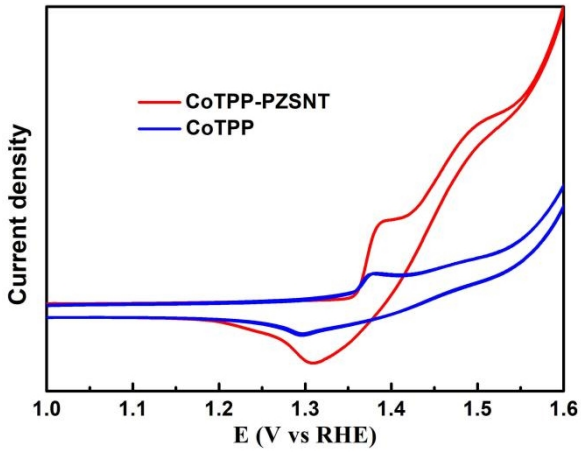

Figure S4. Cyclic voltammograms curves of CoTPP-PZSNT and CoTPP in 1.0 M KOH.

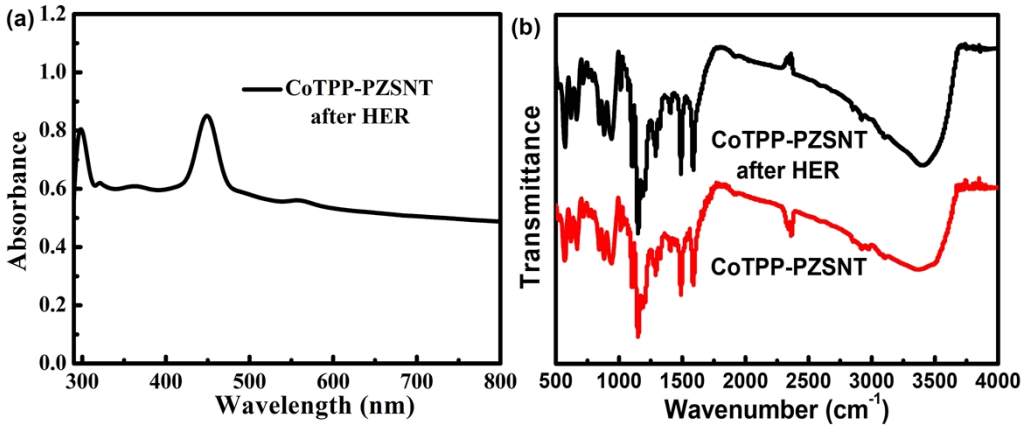

Figure S5. (a) UV-vis absorption and (b) FTIR spectra of CoTPP-PZSNT after HER.

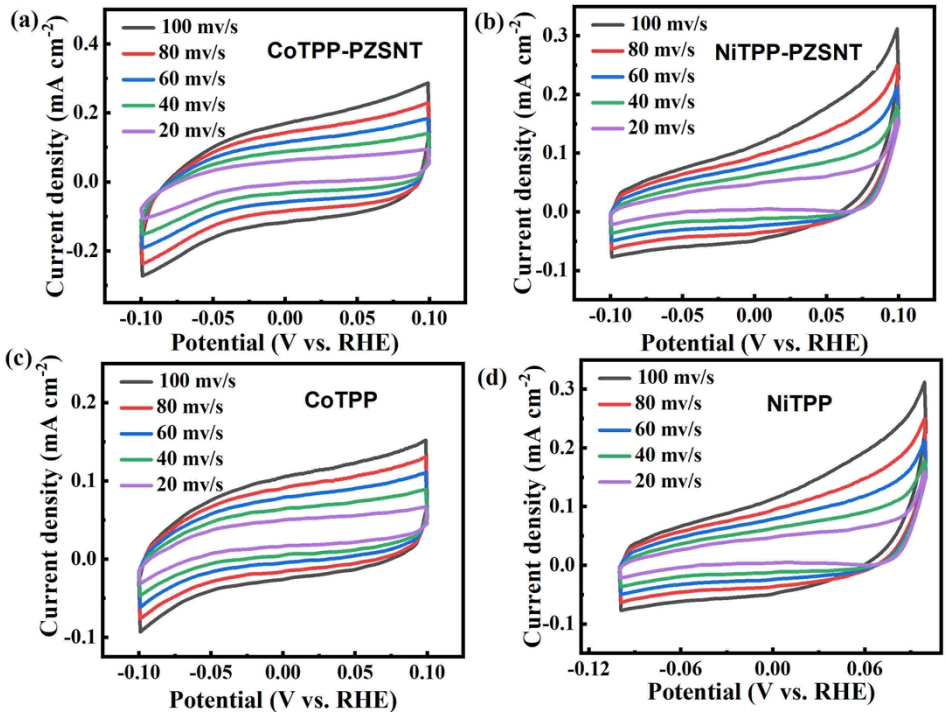

Figure S6. Cyclic voltammograms curves of the samples at different scan rates in 1.0 M KOH.

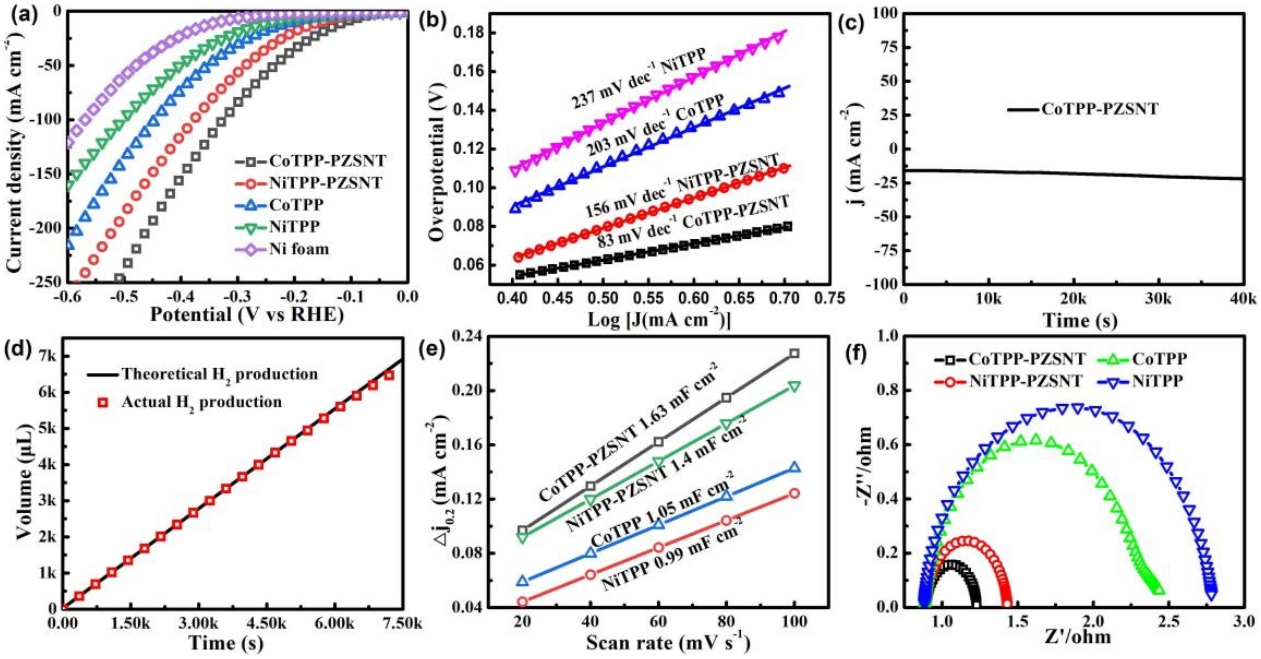

Figure S7. (a) HER LSV curves and (b) Tafel plots of the samples; (c) time-dependent HER stability, (d) Faradaic efficiency of generated H_2 versus theoretical quantity for NiTPP-PZSNT, (e) Capacitive currents at different scan rates and (f) Nyquist plots of the samples.

Table S1. Comparison of HER performance of **CoTPP-PZSNT** with some other reported electrocatalysts.

Electrocatalysts	**Overpotential (mV@10 mA cm^{-2})**	**Refs.**
NiFe LDH	170 (1.0 M KOH)	[1]
NiFe LDH@DG	270 (1.0 M KOH)	[2]
Nb_4C_3Tx-180	263 (1.0 M KOH)	[3]
$Co_{0.85}Se$|NiFe LDH	260 (1.0 M KOH)	[4]
MoS_2|$Ni(OH)_2$	197 (1.0 M KOH)	[5]
B-substituted graphene	200 (1.0 M KOH)	[6]
N doped Graphene	580 (0.5 M H_2SO_4)	[7]
MoO_2 /MoC_2	161 (0.5 M H_2SO_4)	[8]
Ni_xSe_y	225 (0.5 M H_2SO_4)	[9]
MoSSe nanodots	140 (0.5 M H_2SO_4)	[10]
$NiSe_2$@NG	201 (0.5 M H_2SO_4)	[11]
Co-EPOP	173 (0.5 M H_2SO_4)	[12]
C-6-TRZ-TFP COF	200 (0.5 M H_2SO_4)	[13]
NiTPP-PZSNT	**199 (1.0 M KOH)**	**This work**
NiTPP-PZSNT	**151 (0.5 M H_2SO_4)**	**This work**
CoTPP-PZSNT	**157 (1.0 M KOH)**	**This work**
CoTPP-PZSNT	**109 (0.5 M H_2SO_4)**	**This work**

References

1. Gopi, S., K. Giribabu, M. Kathiresan, et al., Cobalt(ii) ions and cobalt nanoparticle embedded porous organic polymers: An efficient electrocatalyst for water-splitting reactions. Sustainable Energy & Fuels. **4** (2020) 3797-3805.
2. He, J., T. Qian, C. Cai, et al., Nickel-based selenides with a fractal structure as an excellent bifunctional electrocatalyst for water splitting. Nanomaterials. **12** (2022) 281.
3. Hou, Y., M. R. Lohe, J. Zhang, et al., Vertically oriented cobalt selenide/nife layered-double-hydroxide nanosheets supported on exfoliated graphene foil: An efficient 3d electrode for overall water splitting. Energy & Environmental Science. **9** (2016) 478-483.
4. Jia, Y., L. Z. Zhang, G. P. Gao, et al., A heterostructure coupling of exfoliated ni-fe hydroxide nanosheet and defective graphene as a bifunctional electrocatalyst for overall water splitting. Advanced Materials. **29** (2017) 1700017.
5. Li, W., B. Yu, Y. Hu, et al., Core-shell structure of nise2

nanoparticles@nitrogen-doped graphene for hydrogen evolution reaction in both acidic and alkaline media. Acs Sustainable Chemistry & Engineering. **7** (2019) 4351-4359.

6. Rajeshichanna, G., T. I. Singh, N. H. Kim, et al., Remarkable bifunctional oxygen and hydrogen evolution electrocatalytic activities with trace-level fe doping in ni- and co-layered double hydroxides for overall water-splitting. Acs Applied Materials & Interfaces. **10** (2018) 42453-42468.
7. Ruidas, S., B. Mohanty, P. Bhanja, et al., Metal-free triazine-based 2d covalent organic framework for efficient H2 evolution by electrochemical water splitting. Chemsuschem. **14** (2021) 5057-5064.
8. Sathe, B. R., X. Zou and T. Asefa, Metal-free b-doped graphene with efficient electrocatalytic activity for hydrogen evolution reaction. Catalysis Science & Technology. **4** (2014) 2023-2030.
9. Tan, C., Z. Luo, A. Chaturvedi, et al., Preparation of high-percentage 1t-phase transition metal dichalcogenide nanodots for electrochemical hydrogen evolution. Advanced Materials. **30** (2018) 1705509.
10. Tan, Y., Z. Zhu, X. Zhang, et al., Nb4C3Tx (mxene) as a new stable catalyst for the hydrogen evolution reaction. International Journal of Hydrogen Energy. **46** (2021) 1955-1966.
11. Zhang, R., X. Xiao, Z. Wang, et al., Heterostructural MoO2/MoC2 microspheres for efficient electrocatalytic hydrogen evolution. Materials Letters. **297** (2021) 129973.
12. Zheng, W., Y. Zhang, K. Niu, et al., Selective nitrogen doping of graphene oxide by laser irradiation for enhanced hydrogen evolution activity. Chemical Communications. **54** (2018) 13726-13729.
13. Zhu, Z., H. Yin, C.-T. He, et al., Ultrathin transition metal dichalcogenide/3d metal hydroxide hybridized nanosheets to enhance hydrogen evolution activity. Advanced Materials. **30** (2018) 1801171.